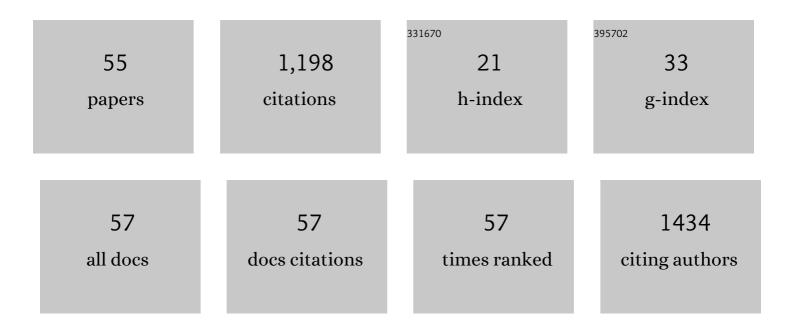
Li-Jun Zhang

List of Publications by Year in descending order

Source: https://exaly.com/author-pdf/2979435/publications.pdf Version: 2024-02-01



#	Article	IF	CITATIONS
1	Highly selective and sensitive sensor based on an organic electrochemical transistor for the detection of ascorbic acid. Biosensors and Bioelectronics, 2018, 100, 235-241.	10.1	103
2	Chirality detection of amino acid enantiomers by organic electrochemical transistor. Biosensors and Bioelectronics, 2018, 105, 121-128.	10.1	73
3	Cannizzaro-Type Disproportionation of Aromatic Aldehydes to Amides and Alcohols by Using Either a Stoichiometric Amount or a Catalytic Amount of Lanthanide Compounds. Journal of Organic Chemistry, 2006, 71, 3149-3153.	3.2	72
4	MicroRNA-139-3p regulates osteoblast differentiation and apoptosis by targeting ELK1 and interacting with long noncoding RNA ODSM. Cell Death and Disease, 2018, 9, 1107.	6.3	64
5	Synthesis, Characterization, Selective Catalytic Activity, and Reactivity of Rare Earth Metal Amides with Different Metalâ^'Nitrogen Bonds. Organometallics, 2009, 28, 3882-3888.	2.3	55
6	A solvent-free synthesis of α,α′-bis(substituted benzylidene) cycloalkanones catalyzed by lanthanide amides [(Me3Si)2N]3Ln(µ-Cl)Li(THF)3 under microwave irradiation. Green Chemistry, 2005, 7, 683.	9.0	47
7	Cyclopentadienylâ€Free Rareâ€Earth Metal Amides [{(CH ₂ SiMe ₂){(2,6â€ <i>i</i> Pr ₂ C ₆ H ₃)N} <sub as Highly Efficient Versatile Catalysts for C–C and C–N Bond Formation. European Journal of Organic Chemistry, 2010, 2010, 326-332.</sub 	>2] 2.4	⊦Ln{N(SiMe≪ 47
8	Synthesis of Bis(NHC)-Based CNC-Pincer Rare-Earth-Metal Amido Complexes and Their Application for the Hydrophosphination of Heterocumulenes. Organometallics, 2015, 34, 4553-4559.	2.3	47
9	Synthesis and Reactivity of Rare-Earth-Metal Monoalkyl Complexes Supported by Bidentate Indolyl Ligands and Their High Performance in Isoprene 1,4-cis Polymerization. Organometallics, 2015, 34, 4251-4261.	2.3	38
10	Copper-Catalyzed Electrophilic Amination of Organoaluminum Nucleophiles with <i>O</i> -Benzoyl Hydroxylamines. Journal of Organic Chemistry, 2015, 80, 6323-6328.	3.2	37
11	MiR-30 family members inhibit osteoblast differentiation by suppressing Runx2 under unloading conditions in MC3T3-E1 cells. Biochemical and Biophysical Research Communications, 2020, 522, 164-170.	2.1	37
12	Synthesis of amides through the Cannizzaro-type reaction catalyzed by lanthanide chlorides. Tetrahedron, 2009, 65, 10022-10024.	1.9	36
13	Rare-Earth Metal Chlorides as Efficient Catalysts for the Simple and Green Synthesis of 1,2-Disubstituted Benzimidazoles and 2-Substituted Benzothiazoles Under Ultrasound Irradiation. Synthetic Communications, 2012, 42, 328-336.	2.1	31
14	Zoophycos macroevolution since 541 Ma. Scientific Reports, 2015, 5, 14954.	3.3	31
15	Synthesis, Characterization, and Catalytic Activity of Some Neodymium(III), Ytterbium(II), and Europium(II) Complexes with Pyrrolidinyl- and Piperidinyl-Functionalized Indenyl Ligands. European Journal of Inorganic Chemistry, 2007, 2007, 1519-1528.	2.0	29
16	Targeted silencing of miRNA-132-3p expression rescues disuse osteopenia by promoting mesenchymal stem cell osteogenic differentiation and osteogenesis in mice. Stem Cell Research and Therapy, 2020, 11, 58.	5.5	28
17	Targeted overexpression of the long noncoding RNA ODSM can regulate osteoblast function in vitro and in vivo. Cell Death and Disease, 2020, 11, 133.	6.3	27
18	Transmetal-Catalyzed Enantioselective Cross-Coupling Reaction of Racemic Secondary Benzylic Bromides with Organoaluminum Reagents. Organic Letters, 2016, 18, 6022-6025.	4.6	26

LI-JUN ZHANG

#	Article	IF	CITATIONS
19	Bone-targeted IncRNA OGRU alleviates unloading-induced bone loss via miR-320-3p/Hoxa10 axis. Cell Death and Disease, 2020, 11, 382.	6.3	25
20	Rareâ€Earth Metal Chlorides Catalyzed Oneâ€pot Syntheses of Quinolines under Solventâ€free Microwave Irradiation Conditions. Chinese Journal of Chemistry, 2013, 31, 465-471.	4.9	23
21	<i>Zoophycos</i> composite ichnofabrics and tiers from the Permian neritic facies in South China and south-eastern Australia. Lethaia, 2010, 43, 182-196.	1.4	21
22	Microchamber-Free Digital Flow Cytometric Analysis of T4 Polynucleotide Kinase Phosphatase Based on Single-Enzyme-to-Single-Bead Space-Confined Reaction. Analytical Chemistry, 2021, 93, 14828-14836.	6.5	19
23	Uppermost Permian trace fossils along a shelf to slope transect in South China and their implications for oceanic redox evolution and extinction pattern. Global and Planetary Change, 2018, 167, 74-86.	3.5	18
24	Early Triassic trace fossils from South China marginal-marine settings: Implications for biotic recovery following the end-Permian mass extinction. Bulletin of the Geological Society of America, 2019, 131, 235-251.	3.3	17
25	Lanthanide Amideâ€catalyzed Azaâ€Henry Reaction of <i>N</i> â€Tosyl Imines with Nitroalkanes. Chinese Journal of Chemistry, 2009, 27, 2061-2065.	4.9	16
26	Synthesis of rare earth metal complexes incorporating amido and enolate mixed ligands: Characterization and reactivity. Polyhedron, 2008, 27, 2757-2764.	2.2	15
27	Rare-earth metal amido complexes supported by bridged bis(β-diketiminato) ligand as efficient catalysts for hydrophosphonylation of aldehydes and ketones. Science China Chemistry, 2013, 56, 329-336.	8.2	15
28	Asymmetric Addition of Pyridyl Aluminum Reagents to Aldehydes Catalyzed by a Titanium(IV) Catalytic System of (<i>R</i>)-H ₈ -BINOLate. Journal of Organic Chemistry, 2015, 80, 8307-8313.	3.2	15
29	Complex behavioural patterns and ethological analysis of the trace fossil <i>Zoophycos</i> : evidence from the Lower Devonian of South China. Lethaia, 2016, 49, 275-284.	1.4	15
30	Early Triassic estuarine depauperate Cruziana Ichnofacies from the Sichuan area of South China and its implications for the biotic recovery in brackish-water settings after the end-Permian mass extinction. Palaeogeography, Palaeoclimatology, Palaeoecology, 2017, 485, 351-360.	2.3	15
31	Lower Devonian tempestites in western Yangtze, South China: insight from <i>Zoophycos</i> ichnofabrics. Geological Journal, 2014, 49, 177-187.	1.3	13
32	Palaeoenvironmental and ecological interpretation of the trace fossil Rhizocorallium based on contained iron framoboids (Upper Devonian, South China). Palaeogeography, Palaeoclimatology, Palaeoecology, 2016, 446, 144-151.	2.3	13
33	Syntheses, Structures, and Catalytic Activities of the Anionic Heterobimetallic Rare-Earth Metal Complexes Supported by Pyrrolyl-Substituted 1,2-Diimino Ligands. Inorganic Chemistry, 2018, 57, 10390-10400.	4.0	13
34	Abundant Zoophycos and Chondrites from the Messinian (Upper Miocene) of northwestern Algeria. Journal of African Earth Sciences, 2020, 171, 103921.	2.0	12
35	Syntheses of Dianionic α-Iminopyridine Rare-Earth Metal Complexes and Their Catalytic Acitivities toward Dehydrogenative Coupling of Amines with Hydrosilanes. Inorganic Chemistry, 2020, 59, 9683-9692.	4.0	11
36	Rare-Earth-Metal-Complex-Catalyzed Hydroalkoxylation and Tandem Hydroalkoxylation/Cyclohydroamination of Isocyanates: Synthesis of Carbamates and Oxazolidinones. Inorganic Chemistry, 2022, 61, 3202-3211.	4.0	10

LI-JUN ZHANG

#	Article	IF	CITATIONS
37	Anti-tumor peptide AP25 decreases cyclin D1 expression and inhibits MGC-803 proliferation via phospho-extracellular signal-regulated kinase-, Src-, c-Jun N-terminal kinase-and phosphoinositide 3-kinase-associated pathways. Molecular Medicine Reports, 2015, 12, 4396-4402.	2.4	9
38	Preformulation Studies and Enabling Formulation Selection for an Insoluble Compound at Preclinical Stage—From InÂVitro, In Silico to InÂVivo. Journal of Pharmaceutical Sciences, 2020, 109, 950-958.	3.3	9
39	The Complete Mitogenome of Pyrrhocoris tibialis (Hemiptera: Pyrrhocoridae) and Phylogenetic Implications. Genes, 2019, 10, 820.	2.4	8
40	Synthesis and Reactivity of NNNNN-Pincer Multidentate Pyrrolyl Rare-Earth-Metal Amido-Chloride or Dialkyl Complexes. Organometallics, 2020, 39, 4525-4534.	2.3	8
41	Periodic fluctuations of marine oxygen content during the latest Permian. Global and Planetary Change, 2020, 195, 103326.	3.5	7
42	Simple Lanthanide Amides [(Me ₃ Si) ₂ N] ₃ Ln(<i>µ</i> â€Cl)Li(THF) ₃ as Highly Efficient Catalysts for the Nitroaldol Reaction. Chinese Journal of Chemistry, 2008, 26, 2267-2272.	4.9	6
43	Syntheses of Rare-Earth Metal Alkyl Complexes Bearing a Dianionic α-Iminopyridyl Ligand and Their Catalytic Activities toward Polymerization of 2-Vinylpyridine. Organometallics, 2021, 40, 3462-3471.	2.3	6
44	Circulating Exosomes from Mice with LPS-Induced Bone Loss Inhibit Osteoblast Differentiation. Calcified Tissue International, 2022, 111, 185-195.	3.1	6
45	The combined effects of simulated microgravity and X-ray radiation on MC3T3-E1 cells and rat femurs. Npj Microgravity, 2021, 7, 3.	3.7	4
46	Syntheses, structures and catalytic activities of lowâ€coordinated rareâ€earth metal complexes containing 2,2′â€pyridylpyrrolides. Applied Organometallic Chemistry, 2020, 34, e5275.	3.5	3
47	Synthesis, Structure, and Reactivity of Monoguanidinate Rare-Earth Metal Aminobenzyl Enolate Complexes. European Journal of Inorganic Chemistry, 2020, 2020, 2153-2164.	2.0	3
48	The small protein MafG plays a critical role in MC3T3-E1 cell apoptosis induced by simulated microgravity and radiation. Biochemical and Biophysical Research Communications, 2021, 555, 175-181.	2.1	3
49	HDAC6 Negatively Regulates miR-155-5p Expression to Elicit Proliferation by Targeting RHEB in Microvascular Endothelial Cells under Mechanical Unloading. International Journal of Molecular Sciences, 2021, 22, 10527.	4.1	3
50	Simulation of External Stray Light for FY-3C VIRR Combined with Satellite Orbit Attitude Model. Remote Sensing, 2021, 13, 5037.	4.0	3
51	Genomeâ€wide gene expression profiles of the pea aphid (Acyrthosiphon pisum) under cold temperatures provide insightsÂinto body color variation. Archives of Insect Biochemistry and Physiology, 2021, 108, e21797.	1.5	2
52	Synthesis, Structure of Zinc Complexes Containing Sulfonylated Binaphtholate Ligands and Their Catalytic Activities towards Ringâ€Opening Polymerization of Lactide and <i>ε</i> â€Caprolactone. Chinese Journal of Chemistry, 2012, 30, 2176-2182.	4.9	1
53	Spatial differentiation of urban carbon emissions — An exploratory spatial data analysis in Beijing. , 2013, , .		1

54 China's economic zoning based on geographic information technology. , 2013, , .

0

#	Article	IF	CITATIONS
55	Morphology and ethology of the Late Devonian trace fossil <i>Rhizocorallium</i> from the Xichuan section of Central China. Lethaia, 2020, 53, 217-228.	1.4	Ο